ISSN 1070-3284, Russian Journal of Coordination Chemistry, 2019, Vol. 45, No. 1, pp. 56–61. © Pleiades Publishing, Ltd., 2019.
Russian Text © M.A. Mikhailov, P.A. Abramov, A.D. Mironova, M.R. Gallyamov, D.G. Sheven', V.V. Pervukhin, M.N. Sokolov, 2019, published in Koordinatsionnaya Khimiya, 2019, Vol. 45, No. 1, pp. 58–64.

Methyl Propiolate Cluster Complex $(Ph_4P)_2[W_6I_8(C{\equiv}C{-}C(O)OCH_3)_6]$

M. A. Mikhailov[a, *], **P. A. Abramov**[a, b], **A. D. Mironova**[a], **M. R. Gallyamov**[a], **D. G. Sheven'**[a], **V. V. Pervukhin**[a], and **M. N. Sokolov**[a, b, c]

[a]*Nikolaev Institute of Inorganic Chemistry, Siberian Branch, Russian Academy of Sciences, Novosibirsk, 630090 Russia*
[b]*Novosibirsk State University, Novosibirsk, 630090 Russia*
[c]*Kazan Federal University, Kazan, 420008 Russia*
**e-mail: mikhajlovmaks@yandex.ru*

Received March 15, 2018; revised June 15, 2018; accepted June 15, 2018

Abstract—A new organometallic iodide cluster complex $(Bu_4N)_2[W_6I_8(C{\equiv}C{-}C(O)OCH_3)_6]$ (**I**), analogous to the previously described $(Bu_4N)_2[Mo_6I_8(C{\equiv}C{-}C(O)OCH_3)_6]$, was obtained by the reaction of $(Bu_4N)_2[W_6I_{14}]$ with silver methyl propiolate $AgC{\equiv}C{-}C(O)OCH_3$. The crystal structure was established for the tetraphenylphosphonium salt $(Ph_4P)_2[W_6I_8(C{\equiv}C{-}C(O)OCH_3)_6]$ (**II**). According to X-ray diffraction (CIF file CCDC no. 1829205), tungsten atoms in **II** are coordinated by terminal carbon atoms of methyl propiolate ligands at W–C distances of 2.220(12)–2.268(14) Å. The methyl propiolate complexes were characterized by electrospray mass spectrometry, ^{1}H and ^{13}C NMR spectroscopy, elemental analysis, and IR spectroscopy.

Keywords: clusters, tungsten, iodides, methyl propiolates, organometallic compounds, crystal structure

DOI: 10.1134/S1070328419010081

INTRODUCTION

The octahedral halide cluster complexes $[\{M_6(\mu_3\text{-}I)\}_8L_6]$ (M = Mo, W; X = I; L = organic or inorganic ligand) possess record high photophysical properties among coordination compounds [1, 2]. These include rather narrow emission band in the red spectral region, visible-light excitation of luminescence, high quantum yields, and high triplet to singlet oxygen conversion. A rather representative range of molybdenum iodide cluster complexes with various terminal ligands L (halides, O-, N-, S-, C-donors) have been synthesized. Several promising applications of luminescent materials and reagents based on molybdenum iodide clusters have been proposed [3–22]. Octahedral tungsten clusters are much less studied than molybdenum clusters, with tungsten iodide clusters being least known. Apart from the expected similarity of the photophysical properties [23], the tungsten iodide clusters attract attention due to relative stability of the paramagnetic 23-electron state (the $[W_6I_{14}]^{2-}$/$[W_6I_{14}]^-$ potential in acetonitrile is only 0.57 V versus the standard calomel electrode [24]) and unique combination of 14 heavy atoms in the $\{W_6I_8\}^{4+}$ cluster core, which ensures high X-ray scattering factor on these atoms. These facts make these cluster complexes promising X-ray contrast agents [25]. Nevertheless, only few octahedral tungsten iodide clusters are known to date. They include, first of all, W_6I_{12}, mixed iodide chloride $W_6I_8Cl_4$ [26, 27], and halides $[\{W_6I_8\}X_6]^{2-}$ (X = Cl, Br, I) [28]. The replacement of terminal iodine atoms affords triflate [25], tosylate [29], and carboxylate complexes, which were studied in detail for photophysical properties [30, 31].

Here we report the preparation of the first organometallic derivative of $\{W_6I_8\}^{4+}$, namely, the propiolate complex $[W_6I_8(C{\equiv}C{-}C(O)OCH_3)_6]^{2-}$, which was isolated and characterized as tetrabutylammonium and tetraphenylphosphonium salts.

EXPERIMENTAL

The starting complex $(Bu_4N)_2[W_6I_{14}]$ was synthesized according to an optimized procedure of [31]. The silver methyl propiolate $AgC{\equiv}C{-}C(O)OCH_3$ was prepared as a white powder by exchange reaction between commercially available $HC{\equiv}C{-}C(O)OCH_3$ and $AgNO_3$ in the presence of Et_3N in an acetonitrile solution [16]. The organic solvents (acetonitrile and dichloromethane) were purified by standard procedures. The syntheses were carried out under argon, and recrystallization can be performed in air.

Synthesis of $(Bu_4N)_2[W_6I_8(C{\equiv}C{-}C(O)OCH_3)_6]$ (I). $(Bu_4N)_2W_6I_{14}$ (0.33 g, 0.10 mmol) was dissolved in CH_2Cl_2 (10 mL) in a small conical flask wrapped with aluminum foil to eliminate the effect of light. A tenfold molar excess of solid $AgC{\equiv}C{-}C(O)OCH_3$ (0.186 g, 0.98 mmol) was added to the resulting light orange solution. The reaction mixture was magnetically stirred for 2 days and filtered through a paper filter. The filtrate was concentrated on a rotary evaporator, and the thick oil thus formed was dissolved in acetonitrile. On slow saturation of acetonitrile with diethyl ether vapor, the product crystallized as light orange crystals. The yield was 30 mg (10%).

For $C_{56}H_{90}N_2O_{12}I_8W_6$

Anal. calcd., %	C, 21.7	H, 2.9	N, 0.9
Found, %	C, 21.5	H, 3.0	N, 1.0

IR (KBr; ν, cm^{-1}): 2958 m, 2873 m, 2234 w, 2089 s, 1865 w, 1678 s, 1511 w, 1478 m, 1456 m, 1430 m, 1378 w, 1209 s, 1108 m, 1059 m, 1006 m, 862 m, 795 w, 756 m, 743 m, 648 w, 554 m. ESI MS (MeCN, *m/z*): average. 1309.1 ($[W_6I_8(C{\equiv}C{-}C(O)OCH_3)_6]^{2-}$; calcd. 1309.0), average 2859.3 ($\{(Bu_4N)[W_6I_8(C{\equiv}C{-}C(O)OCH_3)_6]\}^-$; calcd. 2859.3). ^{13}C NMR ($(CD_3)_2SO$; δ, ppm): 152.14 (C=O group of the ligand), 132.49 and 112.93 (C≡C group of the ligands), 58.47 (Bu_4N^+ cations) 52.58 (OCH_3 group of the ligands), 23.99, 20.14, 14.42 (Bu_4N^+ cations, respectively). ^1H NMR ($(CD_3)_2SO$; δ, ppm, normalized to 24 protons of the Bu_4N^+ CH_3 groups: 3.58 (s., 18 H, OCH_3 groups of the coordinated propiolate).

High-quality single crystals for X-ray diffraction were obtained as Ph_4P salt **II** by diffusion of the diethyl ether vapor into an acetonitrile solution of $(Bu_4N)_2[W_6I_8(C{\equiv}C{-}C(O)OCH_3)_6]$ and Ph_4PBr.

IR spectra were measured on Scimitar FTS 2000 and Specord IR 75 spectrometers in the 4000–400 cm^{-1} range. ^{13}C NMR spectrum was recorded on a Bruker Avance 500 spectrometer at room temperature using $Si(CH_3)_4$ as the internal standard. Elemental analysis was carried out at the analytical laboratory of the Nikolaev Institute of Inorganic Chemistry.

The mass spectrometric data were obtained on an Agilent liquid chromatograph–mass spectrometer (LC/MC) (6130 Quadrupole MS, 1260 infinity LC). Analysis was carried out in the 350–3000 a.m.u. range for both positive and negative ions in the SCAN mode. Electrospray ionization was used. A gaseous nitrogen flow (7 L/min) at a temperature of 350°C served as the drying agen; the nozzle pressure (nitrogen) was 60 psi, and the capillary voltage was 4000 V. In order to retain weakly bound species in the mass spectra, zero fragmentor voltage was used in all experiments. A solution of the test compound (5 μL) in deuterated acetonitrile with a concentration of ~10^{-4} g/mL was introduced into the mobile phase (special purity grade acetonitrile) at a flowrate of 0.4 mL/min, sprayed, and ionized. The experimental peak were compared with calculated ones, in particular, regarding the isotopic distribution. The calculations were carried out using the Molecular Weight Calculator by Matthew Monroe.

X-ray diffraction. The structure of compound **II** was solved by the standard procedure on a Bruker-Apex Duo diffractometer (MoK_α, $\lambda = 0.71073$ Å, graphite monochromator). The reflection intensities were measured by φ- and ω-scanning of narrow (0.5°) frames at $T = 150$ K. The absorption corrections were applied empirically by the SADABS program [32]. The structure was solved by direct methods and refined by full-matrix leas squares method on F^2 in the anisotropic approximation for nonhydrogen atoms by the SHELX 2014\7 algorithm using the ShelXle program [33]. The C≡C bond lengths (1.2 Å) were fixed due to improper absorption corrections used, which accounts for anomalous size of the thermal ellipsoids of carbon atoms. Selected bond lengths in the cluster anion of complex **II** (Å) are summarized in Table 1. The crystal data and structure refinement details for complex **II** are summarized in Table 2. The atom coordinates and other structure parameters are deposited with the Cambridge Crystallographic Data Centre (CCDC no. 1829205; http://www.ccdc.cam.ac.uk/data_request/cif).

RESULTS AND DISCUSSION

The cluster complex salt **I** was prepared by the exchange reaction of $(Bu_4N)_2[W_6I_{14}]$ with the silver salt $AgC{\equiv}C{-}C(O)OCH_3$ in dichloromethane at room temperature, by analogy with the molybdenum cluster $(Bu_4N)_2[Mo_6I_8(C{\equiv}C{-}C(O)OCH_3)_6]$ [16]. The formation of insoluble AgI effected the desired shift of reaction equilibrium. The use of in situ generated $AgC{\equiv}C{-}C(O)OCH_3$ [16] in the exchange reaction does not give any advantages. The product yield does not exceed 10–15%, irrespective of whether $AgC{\equiv}C{-}C(O)OCH_3$ is taken in excess or in a stoichiometric amount (6 equiv.). This is markedly lower than that for the molybdenum cluster; the causes for this difference are unclear. Possibly, the low yield of **I** is attributable to the formation of insoluble by-products as a result of binding of the cluster anions to silver ions, which precipitate together with AgI. Indeed, the ESI mass spectra of some samples exhibited peaks for the $\{Ag[W_6I_8(C{\equiv}C{-}C(O)OCH_3)_6]\}^-$ anions.

An excess of the silver salt relative to the stoichiometric amount (10 equiv. instead of 6 equiv.) promotes more complete and faster reaction, the extent of which is conveniently monitored by electrospray mass spectrometry by measuring the signal corresponding to the molecular dianion of the target compound $[W_6I_8(C{\equiv}C{-}C(O)OCH_3)_6]^{2-}$. The electrospray mass spectrum of an acetonitrile solution of **I** exhibits signals for the doubly charged anion $[W_6I_8(C{\equiv}C{-}C(O)OCH_3)_6]^{2-}$ and for adducts of these species with

Table 1. Selected bond lengths in the cluster anion of complex **II**

Bond	d, Å	Bond	d, Å
W(1)–W(2)	2.6876(7)	I(2)–W(3)	2.8038(10)
W(1)–W(2)^i	2.6934(7)	I(3)–W(1)	2.7951(9)
W(1)–W(3)^i	2.6886(7)	I(3)–W(2)^i	2.8041(9)
W(1)–W(3)	2.6906(7)	I(3)–W(3)^i	2.8144(10)
W(2)–W(3)	2.6767(7)	I(4)–W(1)	2.8123(9)
W(2)–W(3)^i	2.6920(7)	I(4)–W(2)^i	2.8082(10)
I(1)–W(1)	2.7890(9)	I(4)–W(3)	2.8052(10)
I(1)–W(2)	2.8107(9)	C(2)–W(3)	2.247(13)
I(1)–W(3)^i	2.7881(10)	C(3)–W(2)	2.268(14)
I(2)–W(1)	2.7989(9)	C(4)–W(1)	2.220(12)
I(2)–W(2)	2.8155(10)		

* Symmetry codes: ^{i} $-x + 1, -y, -z + 1$.

the tetrabutylammonium cations $\{(Bu_4N)[W_6I_8(C{\equiv}C{-}C(O)OCH_3)_6]\}^-$, for which the theoretical isotopic distributions match well the experimental ones and their "centers of mass" coincide: the peak with m/z = 1309.1 corresponds to $[W_6I_8(C{\equiv}C{-}C(O)OCH_3)_6]^{2-}$ (m/z(calcd.) = 1309.0) and the peak with m/z = 2859.3 corresponds to $\{(Bu_4N){-}[W_6I_8(C{\equiv}C{-}C(O)OCH_3)_6]\}^-$ (m/z(calcd.) = 2859.3). Apart from these intense signals, non-crystallized samples may give rise to minor signals for $[W_6I_8(C{\equiv}C{-}C(O)OCH_3)_5Cl]^{2-}$ and the adduct $\{TBA[W_6I_8(C{\equiv}C{-}C(O)OCH_3)_5Cl]\}^-$ resulting from exchange reaction with CH_2Cl_2 or HCl traces, which are difficult to remove from this solvent. Compounds **I** and **II** are moderately air-stable and are soluble in common organic solvents (except for hydrocarbons).

The ^{13}C NMR spectrum of **I** in $(CD_3)_2SO$ (Fig. 1a) contains signals for the C-coordinated propiolate ligands and tetrabutylammonium cations. The ^{13}C NMR spectrum of $HC{\equiv}C{-}C(O)OCH_3$ in $(CD_3)_2SO$ is shown in Fig. 1b. As can be seen upon comparison of the spectra, the coordination of propiolate ligands changes positions of all signals. The most pronounced (upfield) shift occurs for atoms at the triple bond (δ = 132.49 and 112.93 ppm (C≡C group of coordinated ligands) versus δ = 79.14 and 74.93 ppm (C≡C group of free propiolate)), whereas the (downfield) shifts of the carbonyl and methoxide group signals upon coordination are less pronounced (δ = 152.14 and 52.58 ppm (=C=O and –OMe groups of the coordinated ligands, respectively) and δ = 153.19 and 53.33 ppm (=C=O and –OMe groups of free propiolate)). This is in line with the statement that the greatest electron density change occurs for the carbon atoms at the triple bond due to the formation of the W–C bond and to triple bond conjugation. The chemical shift displacement to the left corresponds to decrease in the electron density on the C≡C atoms and electron density delocalization in the $\{W_6I_8\}^{4+}$ cluster core, which behaves as a strong Lewis acid. The ^1H NMR spectrum of **I** in $(CD_3)_2SO$ shows a signal at δ = 3.58 ppm corresponding to the methoxide protons of the ligands (versus δ = 3.74 ppm for free propiolate) (Fig. 2).

The preparation of single crystals suitable for X-ray diffraction was possible by replacement of the Bu_4N^+ cations by sterically more rigid Ph_4P^+ cations less prone to disorder. This was done by slow saturation of

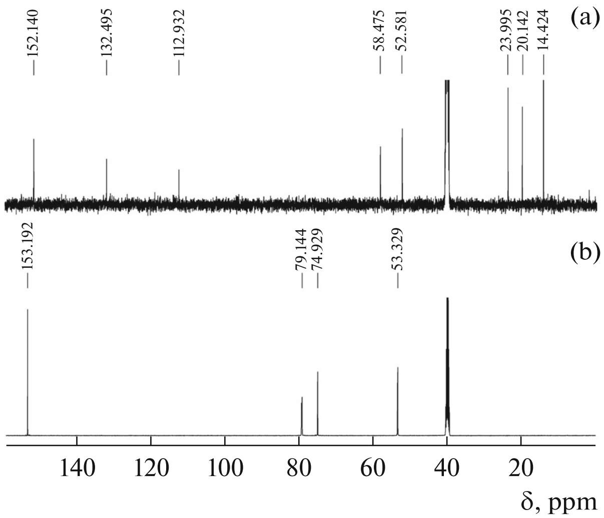

Fig. 1. ^{13}C NMR spectra of solutions: (a) complex **I** in $(CD_3)_2SO$ and (b) $HC{\equiv}C{-}C(O)OCH_3$ in $(CD_3)_2SO$.

Table 2. Crystallographic characteristics and X-ray experiment details for **II**

Parameter	Value
Molecular formula	$C_{72}H_{58}O_{12}P_2I_8W_6$
M	3295.42
Temperature, K	150.0(2)
System	Triclinic
Space group	$P\bar{1}$
a, Å	11.5267(11)
b, Å	13.0563(12)
c, Å	13.4785(15)
α, deg	87.802(4)
β, deg	88.936(4)
γ, deg	75.980(3)
V, Å^3	1966.5 (3)
Z	1
μ, mm^{-1}	11.976
Crystal size (mm)	0.30 × 0.04 × 0.02
Data collection θ range, deg.	1.6–26.4
Ranges of reflection indices	$-14 \leq h \leq 14$, $-16 \leq k \leq 16$, $-16 \leq l \leq 16$
Number of measured reflections	22051
Number of unique reflections (R_{int})	8058 (0.057)
Number of reflections with $I \geq 2\sigma(I)$	4869
Number if refined parameters	451
GOOF	0.98
R_1 (on $\|F\|^2$ for reflections with $I > 2\sigma(I)$)	0.043
wR_2 (on $\|F\|^2$ for all reflections)	0.103
Residual electron density (min/max), e/Å^3	−1.42/1.87

a mixture of **I** and Ph_4PBr in acetonitrile with diethyl ether vapor. According to X-ray diffraction data, the propiolate ligands are coordinated to the cluster core through the terminal triple bond carbon atoms along a straight line. The $[W_6I_8(C{\equiv}C{-}C(O)OCH_3)_6]^{2-}$ anion and the crystal packing of complex **II** are shown in Figs. 3 and 4, respectively. The crystals of **II** are isostructural to the crystals of the cluster $(Ph_4P)_2[Mo_6I_8(C{\equiv}C{-}C(O)OCH_3)_6]$ (**III**) [16].

On going from $\{Mo_6I_8\}^{4+}$ to $\{W_6I_8\}^{4+}$, the M–C distances somewhat increase, from 2.180(5)–2.194(2) (average 2.188) [16] to 2.220(12)–2.268(14) Å (average 2.245) Å (Table 1), respectively. The W–C distances in **II** are longer than the Mo–C distances in **III** or in the organometallic complex with coordinated ethylene in *trans*-$[\{Mo_6Cl_8\}Cl_2(C_2H_5)_2(PBu_3)_2] \cdot 2PhCH_3$ (2.21(3) Å) [34] and are comparable with the Mo–C distance in the complex with coordinated benzyl ligands in *trans*-$[\{Mo_6Cl_8\}(PBu_3)_2(CH_2Ph)_4]$ (2.239(14)–2.271(15) Å)

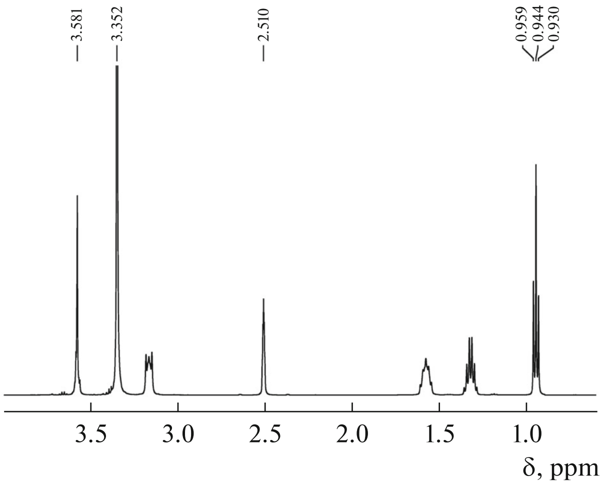

Fig. 2. ^1H NMR spectrum of a solution of complex **I** in $(CD_3)_2SO$. The proton chemical shifts (δ, ppm): CH_3O groups of propiolate ligands (3.58), water (3.35), solvent (2.51 ppm), and methyl groups of the Bu_4N^+ cations (the triplet on the right centered at 0.94 ppm). The other chemical shifts correspond to protons of three methylene groups of tetrabutylammonium.

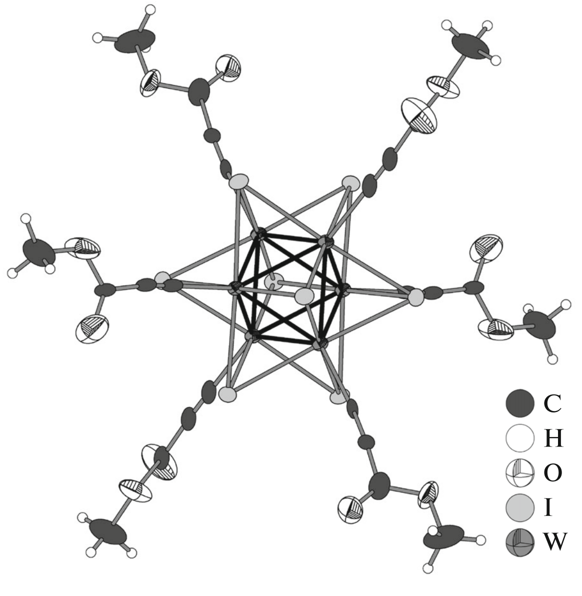

Fig. 3. Structure of the cluster anion $[W_6I_8(C{\equiv}C{-}C(O)OCH_3)_6]^{2-}$ (thermal ellipsoids at 50% probability level).

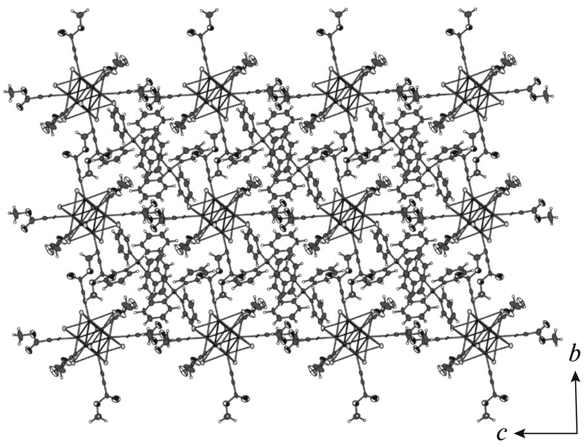

Fig. 4. Crystal packing of complex **II**.

[35]. The preparation of thermally stable, but light sensitive organometallic cluster complexes *trans*-$[\{W_6Cl_8\}Cl_2(C_2H_5)_2(PR_3)_2]$ (R = n-C_4H_9, n-C_5H_{11}) and *trans,mer*-$[\{W_6Cl_8\}Cl(C_2H_5)_3(PR_3)_2]$ (R = n-C_4H_9, n-C_5H_{11}) with η^1-coordinated ethylene (according to ^{13}C NMR) was reported; however, the complexes were not studied by X-ray diffraction [36]. The W–W and W–(μ_3-I) distances of the cluster cores of **II** are characteristic of the $\{W_6I_8\}^{4+}$ cores of the complexes $[\{W_6I_8\}L_6]$ with various ligand natures [24–31] and are given in Table 1.

Thus, we prepared the first organometallic derivative for octahedral tungsten halide clusters.

ACKNOWLEDGMENTS

This work was supported by the Federal Agency of Scientific Organizations of Russia (Program FNI, clause V.44.4.5).

REFERENCES

1. Sokolov, M.N., Mihailov, M.A., Peresypkina, E.V., et al., *Dalton Trans.*, 2011, vol. 40, p. 6375.
2. Elistratova, J., Mikhailov, M., Burilov, V., et al., *RSC Adv.*, 2014, vol. 4, p. 27922.
3. Kirakci, K., Kubat, P., Dusek, M., et al., *Eur. J. Inorg. Chem.,* 2012, p. 3107.
4. Efremova, O.A., Shestopalov, M.A., Chirtsova, N.A., et al., *Dalton Trans.*, 2014, vol. 43, p. 6021.
5. Kirakci, K., Šícha, V., Holub, J., et al., *Inorg. Chem.*, 2014, vol. 53, p. 13012.
6. Kirakci, K., Fejfarová, K., Kučeráková, M., and Lang, K., *Eur. J. Inorg. Chem.*, 2014, p. 2331.
7. Cordier, S., Grasset, F., Molard, Y., et al., *J. Inorg. Organomet. Polym. Mater.*, 2015, vol. 25, p. 189.
8. Elistratova, J., Burilov, V., Mustafina, A., et al., *Polymer*, 2015, vol. 72, p. 98.
9. Prevot, M., Amela-Cortes, M., Manna, S.K., et al., *J. Mater. Chem.*, 2015, vol. 3, p. 5152.
10. Amela-Cortes, M., Paofai, S., Cordier, S., et al., *Chem. Commun.*, 2015, vol. 51, p. 8177.
11. Prevot, M., Amela-Cortes, M., Manna, S.K., et al., *Adv. Funct. Mater.*, 2015, vol. 25, p. 4966.
12. Robin, M., Kuai, W., Amela-Cortes, M., et al., *ACS Appl. Mater. Interfaces*, 2015, vol. 7, p. 21975.
13. Solovieva, A.O., Vorotnikov, Y.A., Trifonova, K.E., et al., *J. Mater. Chem.*, 2016, vol. 4, p. 4839.
14. Kirakci, K., Kubát, P., Fejfarová, K., et al., *Inorg. Chem.*, 2016, vol. 55, p. 803.
15. Vorotnikov, Y.A., Efremova, O.A., Vorotnikova, N.A., et al., *RSC Adv.*, 2016, vol. 6, p. 43367.
16. Sokolov, M.N., Mikhailov, M.A., Brylev, K.A., et al., *Inorg. Chem.*, 2013, vol. 52, p. 12477.
17. Sokolov, M.N., Mikhailov, M.A., Virovets, A.V., et al., *Russ. Chem. Bull.*, 2013, vol. 62, p. 1764.
18. Mikhailov, M.A., Brylev, K.A., Abramov, P.A., et al., *Inorg. Chem.*, 2016, vol. 55, p. 8437.
19. Mikhailov, M.A., Brylev, K.A., Virovets, A.V., et al., *New J. Chem.*, 2016, vol. 40, p. 1162.
20. Beltran, A., Mikhailov, M., Sokolov, M.N., et al., *J. Mater. Chem. B*, 2016, vol. 4, p. 5975.
21. Felipe-Leon, C., Arnau del Valle, C., Perez-Laguna, V., et al., *J. Mater. Chem. B*, 2017, vol. 5, p. 6058.
22. Mikhaylov, M.A., Abramov, P.A., Komarov, V.Yu., and Sokolov, M.N., *Polyhedron*, 2017, vol. 122, p. 241.
23. Zietlow, T.C., Schaefer, W.P., Sadeghi, B., et al., *Inorg. Chem.*, 1986, vol. 25, p. 2195.
24. Mussell, R.D. and Nocera, D.G., *Inorg. Chem.*, 1990, vol. 29, p. 3711.
25. Franolic, J.D., Long, J.R., and Holm, R.H., *J. Am. Chem. Soc.*, 1995, vol. 117, p. 8139.
26. Strobele, M. and Meyer, H.-J., *Inorg. Chem.*, 2017, vol. 56, p. 5880.

27. Strobele, M., Enseling, D., Jüstel, T., and Meyer, H.-J., *Z. Anorg. Allg. Chem.*, 2016, vol. 642, p. 1435.
28. Hogue, R.D. and Mccarley, R.E., *Inorg. Chem.*, 1970, vol. 9, p. 1354.
29. Mikhailov, M.A., Gushchin, A.L., Gallyamov, M.R., et al., *Russ. J. Coord. Chem.*, 2017, vol. 43, p. 172.
30. Riehl, L., Seyboldt, A., Ströbele, M., et al., *Dalton Trans.*, 2016, vol. 45, p. 15500.
31. Sokolov, M.N., Brylev, K.A., Abramov, P.A., et al., *Eur. J. Inorg. Chem.*, 2017, p. 4131.
32. Sheldrick, G.M., *SADABS*, Göttingen: Univ. of Göttingen, 1996.
33. Hübschle, C.B., Sheldrick, G.M., and Dittrich, B., *J. Appl. Crystallogr.*, 2011, vol. 44, p. 1281.
34. Saito, T., Nishida, M., Yamagata, T., et al., *Inorg. Chem.*, 1986, vol. 25, p. 1111.
35. Yamagata, T., Okiyama, H., Imoto, H., and Saito, T., *Acta Crystallogr., Sect. C: Cryst. Struct. Commun.*, 1997, vol. 53, p. 859.
36. Saito, T., Manabe, H., Yamagata, T., and Imoto, H., *Inorg. Chem.*, 1987, vol. 26, p. 1362.

Translated by Z. Svitanko